PNAS Nexus, 2024, 3, pgae371
https://doi.org/10.1093/pnasnexus/pgae371
Advance access publication 27 August 2024
Research Report

Inflammatory signature-based theranostics for acute lung injury in acute type A aortic dissection

Hong Liu [a,*], Yi-fei Diao[a], Si-chong Qian[b], Yong-feng Shao[a], Sheng Zhao[a], Hai-yang Li[b] and Hong-jia Zhang[b]

[a]Department of Cardiovascular Surgery, The First Affiliated Hospital of Nanjing Medical University, Nanjing 2100299, P.R. China
[b]Department of Cardiovascular Surgery, Beijing Anzhen Hospital, Capital Medical University, Beijing 100029, P.R. China
*To whom correspondence should be addressed: Email: dr.hongliu@foxmail.com
Edited By Bruce Levine

Abstract

Acute lung injury (ALI) is a serious adverse event in the management of acute type A aortic dissection (ATAAD). Using a large-scale cohort, we applied artificial intelligence-driven approach to stratify patients with different outcomes and treatment responses. A total of 2,499 patients from China 5A study database (2016–2022) from 10 cardiovascular centers were divided into 70% for derivation cohort and 30% for validation cohort, in which extreme gradient boosting algorithm was used to develop ALI risk model. Logistic regression was used to assess the risk under anti-inflammatory strategies in different risk probability. Eight top features of importance (leukocyte, platelet, hemoglobin, base excess, age, creatinine, glucose, and left ventricular end-diastolic dimension) were used to develop and validate an ALI risk model, with adequate discrimination ability regarding area under the receiver operating characteristic curve of 0.844 and 0.799 in the derivation and validation cohort, respectively. By the individualized treatment effect prediction, ulinastatin use was significantly associated with significantly lower risk of developing ALI (odds ratio [OR] 0.623 [95% CI 0.456, 0.851]; $P = 0.003$) in patients with a predicted ALI risk of 32.5–73.0%, rather than in pooled patients with a risk of <32.5 and >73.0% (OR 0.929 [0.682, 1.267], $P = 0.642$) (Pinteraction = 0.075). An artificial intelligence-driven risk stratification of ALI following ATAAD surgery were developed and validated, and subgroup analysis showed the heterogeneity of anti-inflammatory pharmacotherapy, which suggested individualized anti-inflammatory strategies in different risk probability of ALI.

Keywords: extreme gradient boosting, type A aortic dissection, acute lung injury, risk prediction, inflammation

Significance Statement

Acute lung injury (ALI) is a serious adverse event after acute type A aortic dissection surgery. We developed a computational method that can use these laboratory biomarkers to determine whether a person is at increased risk of developing an ALI. This could enable regular monitoring of these people and might enable ALI to be prevented in some individuals.

Introduction

Acute type A aortic dissection (ATAAD) is a severe cardiovascular disease associated with major morbidity and mortality (1, 2). Despite improvements in surgical techniques and perioperative management strategies, the extremely complex and multifaceted factors including the dissected aorta itself, contrast media for computed tomography angiography, massive blood transfusion, deep hypothermia, cardiopulmonary bypass, serious ischemia–reperfusion injury due to lower body circulatory arrest, and exogenous graft implantation, as well as surgical trauma, anesthesia, mechanical ventilation together initiates serious systemic inflammatory response (3–5), deteriorating acute lung injury (ALI), and likely progressing to multiple organ dysfunction syndrome and even mortality (6). Therefore, early identification of patients at high risk of developing ALI after ATAAD is highly important to facilitate early interventions and medical care.

Several strategies have been suggested for treatment of ALI in ATAAD, of which anti-inflammatory pharmacotherapeutics plays an important protective role (7). Ulinastatin, a glycoprotein acting as a urinary trypsin inhibitor, has been proven to have anti-inflammatory activity by inhibiting the release of pro-inflammatory cytokines and elastase from macrophages and neutrophils to suppress the systemic inflammatory response, resulting in attenuation of ALI (8, 9). Yet, translating group-level estimates of trials to individual patients is challenging, as average measures implicitly consider that all patients have an average risk and the same average response to treatment. Absolute treatment effects, however, can vary substantially among individuals. Individualized prediction of treatment effects provides a comprehensive approach to identify

Competing Interest: The authors declare no competing interests.
Received: April 8, 2024. **Accepted:** August 15, 2024

those patients who benefit most from Ulinastatin, enabling clinicians to make patient-tailored treatment decisions and better weigh treatment benefits against harms (10).

In the present analyses, we aimed to develop and validate a model with patient characteristics, for individualized prediction of the effects of Ulinastatin on ALI after ATAAD surgery, to investigate whether distinct risk stratification groups respond differently to anti-inflammatory pharmacotherapy based on a large-scale cohort of the Chinese ATAAD population.

Methods

Study population

The 5A cohort study (Additive Anti-inflammatory Action for Aortopathy and Arteriopathy) is a national prospective registry involving patients with aortic dissection, who were consecutively enrolled at 10 cardiovascular centers in China (see Supplementary Method). Further details about the China 5A registry are available in our previous study protocol (11). This study focused on patients with ATAAD who underwent surgical repair from 2016 January 1 to 2022 June 30. These patients had documented biomarkers of interest within 6 h of hospital admission, as recorded in the 5A database (12). The study adhered to the Declaration of Helsinki and was registered with ClinicalTrials.gov (NCT04398992). The Institutional Review Board (IRB) of the Aortic Collaborative Institutions approved the study protocol (2021-SR-381), which waived the requirement for written patient consent because of the nature of the retrospective study. The patient cohort was randomly divided into a training set ($N1 = 1{,}749$; 70%) and a test set ($N2 = 750$; 30%). The study followed the Transparent Reporting of a Multivariable Prediction Model for Individual Prognosis or Diagnosis (TRIPOD) Guidelines (13).

Data recourse

Data collections mainly included these characteristics regarding demography, clinical factors, dissection, circulation characteristics, biomarkers, procedural variables, and perioperative outcomes. In particular, clinically available biomarkers were collected within 6 h prior to surgery, including peripheral blood leukocyte (× 109/L), platelet (× 109/L), hemoglobin (g/L), creatine kinase-MB (ng/mL), lactic dehydrogenase (U/L), alanine transaminase (U/L), aspartate aminotransferase (U/L), albumin (g/L), blood urea nitrogen (mmol/L), creatinine (μmoI/L), activated partial thromboplastin time (s), international normalized ratio, arterial pH, $PaCO_2$ (mmHg), base excess (mmol/L), glucose (mmol/L), and lactate (mmol/L). Surgery-related procedures were described as previously reported (14).

Anti-inflammatory pharmacotherapy

Ulinastatin (TECHPOOL Biopharma Co., Ltd., Guangzhou, China) was injected intravenously following institutional protocol starting right after the surgery until intensive care unit (ICU) discharge. Because this is a retrospective study, the actual ulinastatin usage and dosage mainly depended on medicine specification (100,000 U once every 8 h).

Outcomes

Considering the Berlin definition of acute respiratory distress syndrome (15) and American Thoracic Society workshop report (16) as well as the institutional protocol, the primary outcome ALI was defined as radiological evidence of bilateral infiltrates, evidence of physiologic dysfunction (hypoxemia, arterial oxygen tension/fraction inspired oxygen <200 mmHg), and the absence of left atrial hypertension, occurring within 72 h subsequent to the operation, regardless of mechanical ventilation status. Secondary outcomes included 30-day mortality, inhospital mortality, mechanical ventilation duration, ICU length of stay, and hospital length of stay.

Model derivation and validation

The final cohort was randomly divided into a derivation cohort (70%) and a validation cohort (30%). The eXtreme Gradient Boosting (XGBoost) algorithm was selected for model derivation (11, 17). To allow for interpretation of our model's predictions, we used SHapley additive explanation (SHAP) to evaluate key feature importance with identification of a predictor's relative contribution for each observation and averaged across observations to the final prediction (18). Discrimination performance was assessed via the area under the receiver operating characteristic curve (AUROC) and the area under precision-recall curve (AUPRC) (19). Calibration ability was assessed via the calibration plot. Clinical utility was assessed using decision curve analysis (20).

Subgroup analysis

Patients were stratified according to the presence or absence of ulinastatin use. Cubic spline curve analysis was applied to fit the functional relationship of the predicted risk probability as a continuous variable with the primary outcome. Subsequently, we divided patients into three subgroups on the basis of their risk probability (<32.5, 32.5–73.0, and >73.0%) and further tested whether there were interactions between anti-inflammatory pharmacotherapy (ulinastatin) and operative mortality across subgroups of these risk differences. Alluvial plots were created to visualize risk stratification of ALI (low, intermediate, and high risk), anti-inflammatory pharmacotherapy (the absence vs. presence of ulinastatin), and primary outcome (non-ALI vs. ALI), in which a thicker ribbon indicates that a greater number of subjects fell into a particular risk stratification or range. Risk–benefit assessment was performed in subgroups stratified according to surgical strategy based on the number needed to treat (NNT) or the number needed to harm (NNH) measures. Of note, to alleviate the effects of the potential confounding factors as soon as possible, multivariable analysis with adjustment for baseline, clinical procedural factors was employed to investigate the association between ulinastatin use and ALI.

Sample size and power calculation

For binary outcome measures, we proposed that at least 10 events (i.e. patients with the defined outcome) per variable are necessary to avoid overfitting. This effective sample size was achieved in both the derivation cohort, which had 576 events for eight variables, and the validation cohort, with 245 events for the same number of variables.

Statistical analysis

Continuous data are presented as medians with interquartile ranges (IQRs), while categorical data are reported as percentages. We used binary logistic regression to evaluate odds ratios (ORs) and 95% CIs. Features with more than 20% missing values were excluded from the analysis. To handle missing data, we used multiple imputations with chained equations. All statistical analyses were conducted using R version 3.6.1 and Python version 3.6.

Patient and public involvement

No patients or members of the public were involved in determining the research question, outcome measures, or interpreting the

Table 1. Baseline and clinical characteristics and perioperative outcomes of two cohorts.

	Derivation cohort (N1 = 1,749)	Validation cohort (N2 = 750)	Overall (N = 2,499)	P value
Demographic characteristics				
Age (years)	51 (41–59)	50 (42–58)	51 (41–59)	0.468
Sex (male)	1,299 (74.3%)	575 (76.7%)	1,874 (75.0%)	0.205
Height (cm)	171 (165–175)	172 (167–176)	171 (165–176)	0.074
Weight (kg)	75 (65–84)	75 (65–85)	75 (65–85)	0.640
Body mass index (kg/m^2)	25.4 (23.1–27.8)	25.4 (22.8–27.8)	25.4 (23.0–27.8)	0.504
Clinical characteristics				
Time onset to operation (days)	1 (1–2)	1 (1–2)	1 (1–2)	0.876
Heart rate (bpm)	80 (76–88)	80 (75–88)	80 (76–88)	0.271
Diastolic blood pressure (mmHg)	75 (68–80)	73 (65–80)	75 (67–80)	0.026
Systolic blood pressure (mmHg)	130 (120–140)	130 (120–140)	130 (120–140)	0.986
Mean blood pressure (mmHg)	93 (85–100)	93 (85–98)	93 (85–100)	0.155
Smoking *n* (%)	738 (42.8%)	334 (45.5%)	1,072 (43.6%)	0.209
Drinking *n* (%)	344 (20.4%)	173 (24.1%)	517 (21.5%)	0.044
Chronic lung disease *n* (%)	37 (2.1%)	23 (3.1%)	60 (2.4%)	0.154
Coronary heart disease *n* (%)	164 (9.4%)	80 (10.7%)	244 (9.8%)	0.317
Hypertension *n* (%)	1,249 (71.9%)	526 (70.5%)	1,775 (71.5%)	0.493
Diabetes *n* (%)	90 (5.1%)	41 (5.5%)	131 (5.2%)	0.742
Arrhythmias *n* (%)	46 (2.6%)	17 (2.3%)	63 (2.5%)	0.593
Congestive heart failure *n* (%)	4 (0.2%)	6 (0.8%)	10 (0.4%)	0.038
Marfan syndrome *n* (%)	26 (1.5%)	6 (0.8%)	32 (1.3%)	0.161
Home pharmacological treatments				
Statins *n* (%)	254 (14.5%)	113 (15.1%)	367 (14.7%)	0.771
Beta-blockers *n* (%)	281 (16.6%)	98 (13.0%)	379 (15.2%)	0.063
Metformin *n* (%)	42 (2.4%)	21 (2.8%)	63 (2.5%)	0.657
Aspirin *n* (%)	77 (4.4%)	41 (5.4%)	118 (4.7%)	0.295
Dissection characteristics				
Malperfusion[a] *n* (%)	560 (32.0%)	215 (28.7%)	775 (31.0%)	0.097
Circulation characteristics				
Aortic regurgitation *n* (%)				0.801
Mild	553 (33.6%)	230 (32.3%)	783 (33.2%)	
Moderate	215 (13.1%)	96 (13.5%)	311 (13.2%)	
Severe	339 (20.6%)	158 (22.2%)	497 (21.1%)	
Pericardial effusion *n* (%)				0.670
Mild	161 (9.3%)	61 (8.2%)	222 (8.9%)	
Moderate	30 (1.7%)	17 (2.3%)	47 (1.9%)	
Severe	14 (0.8%)	6 (0.8%)	20 (0.8%)	
Pleural effusion *n* (%)				0.927
Minor	65 (3.7%)	30 (4.0%)	95 (3.8%)	
Major	27 (1.5%)	11 (1.5%)	38 (1.5%)	
LVEDD (mm)	50 (46–55)	50 (46–55)	50 (46–55)	0.836
LVEF (%)	62 (59–66)	62 (59–66)	62 (59–66)	0.899
LVESD (mm)	33 (30–37)	33 (30–37)	33 (30–37)	0.309
Biomarkers				
Leukocyte (× 109/L)	8.4 (6.1–12.0)	8.6 (6.2–11.7)	8.5 (6.2–11.9)	0.927
Platelet (× 109/L)	194 (157–239)	192 (157–232)	193 (157–236)	0.470
Hemoglobin (g/L)	138 (125–149)	139 (126–151)	139 (126–150)	0.050
Creatine kinase-MB (ng/mL)	1.3 (0.8–2.2)	1.3 (0.8–2.2)	1.3 (0.8–2.2)	0.484
Lactic dehydrogenase (U/L)	195 (165–237)	197 (164–245)	196 (165–239)	0.244
Alanine transaminase (U/L)	19 (14–30)	19 (14–30)	19 (14–30)	0.819
Aspartate aminotransferase (U/L)	20 (16–26)	20 (16.0–26.0)	20 (16–26)	0.632
Albumin (g/L)	40.4 (37.1–43.2)	40.5 (37.4–43.3)	40.4 (37.2–43.2)	0.557
Blood urea nitrogen (mmol/L)	5.8 (4.7–7.4)	6.0 (4.7–7.4)	5.9 (4.7–7.4)	0.594
Creatinine (μmoI/L)	74.3 (61.9–89.8)	75.9 (63.5–91.5)	74.9 (62.4–90.5)	0.106
INR	1.07 (1.01–1.15)	1.06 (1.00–1.15)	1.07 (1.01–1.15	0.167
APPT (s)	30.4 (28.2–32.9)	30.6 (28.2–33.0)	30.5 (28.2–32.9)	0.635)
PH	7.42 (7.40–7.44)	7.42 (7.40–7.44)	7.42 (7.40–7.44)	0.325
$PaCO_2$ (mmHg)	35.1 (32.1–38.0)	35.1 (32.1–38.3)	35.1 (32.1–38.1)	0.666
Base excess (mmol/L)	−0.7 (−2.0 to 0.8)	−0.7 (−1.9 to 1.0)	−0.7 (−2.0 to 0.8)	0.400
Glucose (mmol/L)	6.0 (5.0–7.4)	5.9 (5.0–7.4)	6.0 (5.0–7.4)	0.930
Lactate (mmol/L)	1.4 (1.0–1.9)	1.3 (1.0–1.9)	1.4 (1.0–1.9)	0.830
Procedural variables				
Root procedure				0.070
Aortic root repair (%)	36 (2.1%)	12 (1.6%)	48 (1.9%)	
Aortic valve replacement (%)	73 (4.2%)	18 (2.4%)	91 (3.6%)	
Aortic root replacement (%)	671 (38.4%)	315 (42.0%)	986 (39.5%)	
Bentall (%)	628 (35.9%)	287 (38.3%)	915 (36.6%)	0.262
David (%)	23 (1.3%)	13 (1.7%)	36 (1.4%)	0.419
Total arch replacement + FET implantation (%)	851 (48.7%)	344 (45.9%)	1,195 (47.8%)	0.201
Hemi-arch replacement (%)	220 (12.6%)	84 (11.2%)	304 (12.2%)	0.196
Total arch replacement (%)	864 (49.4%)	353 (47.1%)	1,217 (48.7%)	0.285

(*continued*)

Table 1. Continued

	Derivation cohort (N1 = 1,749)	Validation cohort (N2 = 750)	Overall (N = 2,499)	P value
Inclusion technique (%)	1,256 (71.8%)	521 (69.5%)	1,777 (71.1%)	0.236
Concomitant CABG (%)	134 (7.7%)	62 (8.3%)	196 (7.8%)	0.606
Concomitant valve surgery (%)	77 (4.4%)	37 (4.9%)	114 (4.6%)	0.560
Cardiopulmonary bypass time (min)	172 (136–206)	168 (134–201)	171 (136–205)	0.252
Aortic cross-clamp time (min)	99 (77–123)	98 (77–121)	98 (77–123)	0.633
Circulatory arrest time (min)	23 (18–29)	23 (18–30)	23 (18–30)	0.276
Anti-inflammatory pharmacotherapy				
Ulinastatin therapy	675 (38.6%)	310 (41.3%)	985 (39.4%)	0.199
Perioperative outcomes				
Acute lung injury (%)	576 (32.9%)	245 (32.7%)	821 (32.9%)	0.897
30-day mortality (%)	71 (4.1%)	26 (3.5%)	97 (3.9%)	0.482
Inhospital mortality (%)	78 (4.5%)	31 (4.1%)	109 (4.4%)	0.714
Mechanical ventilation time (h)	18 (14–38)	18 (14–36)	18 (14–37)	0.664
ICU stay (h)	29 (19–63)	28 (18–65)	29 (19–64)	0.767
Hospital stay (days)	16 (12–22)	15 (11–21)	16 (11–21)	0.308

Data are *n* (%) or median (IQR), unless otherwise specified.
APTT, activated partial thromboplastin time; LVEDD, left ventricular end-diastolic dimension; LVESD, left ventricular end-systolic dimension; LVEF, left ventricular ejection fraction; INR, international normalized ratio; APTT, activated partial prothrombin time; FET, frozen elephant trunk; CABG, coronary artery bypass grafting; ICU, intensive care unit.
[a]Defined as one of the following conditions: coronary malperfusion, renal malperfusion, cerebral perfusion, spinal/lumbar, and intestinal and limb ischemia.

results as this was a doctoral student project without funding to support patient and public involvement. The results of this study will be summarized for the public in a blog post by the first authors on publication, disseminated on the Chinese 5A Alliance websites to their relevant audiences, and publicized on social media.

Results

Patient characteristics and outcomes

There were 2,499 ATAAD patients included for final analysis: 1,749 (70%) in the derivation cohort and 750 (30%) in the validation cohort (Fig. S1). Among overall patients, the median age was 51 (IQR 41–59) years, 1,874 (75.0%) were male, and the median body mass index was 25.4 (IQR 23.0–27.8) kg/m^2. Of these patients, 560 (32.0%) presented with one of the following conditions: coronary malperfusion, renal malperfusion, cerebral malperfusion, intestinal malperfusion, or any pulse deficit/limb ischemia. Baseline, clinical, laboratory, and procedural features of derivation, validation, and overall cohort are reported in Table 1. There were no significant differences in baseline, clinical, laboratory, and procedural features between two cohorts. In derivation cohort, 576 patients developed ALI who were older, obese, higher percentage of hypertension and arrhythmias, higher percentage of malperfusion compared with those without ALI (Table 2).

The incidence of ALI was 32.9, 32.9, and 32.7% in derivation, validation, and overall cohort, respectively. The incidence of 30-day and operative mortality among overall patients was 3.9 and 4.4%, respectively (Table 1). Among the derivation cohort, ALI patients had higher percentage of 30-day and operative mortality, and longer mechanical ventilation time, ICU length of stay, and hospital length of stay than those without ALI (Table 2). Univariate analysis of ALI in overall population was showed in Table S1.

Model characteristics: discrimination, calibration, and clinical use

The SHAP analysis showed the candidate predictor's relative contribution, either positively or negatively, to the prediction of ALI (Fig. 1A–C), which we used to develop a full model to predict ALI, with an AUROC of 0.971 and AUPRC of 0.945 as well as good calibration and clinical utility (Fig. 2 and Table S2). To improve the model's practical application, we selected features that were most strongly associated with the systemic effects of the anti-inflammatory strategy based on a SHAP feature importance of 0.030 or higher, which identified the top eight features: leukocyte, platelet, hemoglobin, base excess, age, creatinine, glucose, and left ventricular end-diastolic dimension (Figs. 1 and S1). By entering these eight indicators, clinicians can easily obtain the appropriate risk probability for a single patient to support decision-making based on an online browser accessible version available for external use (http://www.empowerstats.net/pmodel/? m=7473_ALI) (Fig. 1D).

The selected ALI risk model had high discrimination in development and validation populations, with AUROCs of 0.844 and 0.799, respectively. This inflammatory risk model had adequate accuracy in both the derivation and validation populations, with AUPRC values of 0.764 and 0.696 (Figs. 2 and 3), respectively. There was good calibration and clinical utility in the derivation and validation cohort, respectively (Fig. 2). The other performances of these three risk models were showed in Tables S3 and S4.

Association between ulinastatin use and ALI

Among the 1,749 patients in the derivation cohort, patients with ulinastatin use were less likely to develop ALI than patients without ulinastatin use (375/1,074 [34.9%] vs. 201/675 [29.8%]), Risk difference 0.11 (95% CI 0.01, 0.21), crude OR 0.790 (95% CI 0.642, 0.972, $P = 0.026$) (Table 3). The multivariable analysis confirmed the significant association between ulinastatin use and ALI (adjusted OR 0.666; 95% CI 0.530, 0.836, $P = 0.0005$) with adjustment for procedural factors (root procedure, arch procedure, and concomitant procedure, as well as cardiopulmonary bypass time, and aortic cross-clamp time, and circulatory arrest time). However, there were no significant differences in 30-day and operative mortality between ulinastatin use and no use (all $P > 0.05$) (Table 3).

Subgroup analysis

Alluvial plot showed distribution of risk stratification of ALI (low, intermediate, and high risk) across ulinastatin use and ALI in derivation data (Fig. 3A). The risk model was then used to predict ALI risk for the derivation cohort and plotted against observed risk (Fig. 3B), in which the spline curves for the effect of ulinastatin use vs. no use on the occurrence of ALI mainly across 32.5 and 73.0% from the perspective of clinical significance. By analysis of individual risk probability and treatment effect, ulinastatin use was significantly

Table 2. Baseline and clinical characteristics and perioperative outcomes of ALI vs. non-ALI patients in derivation cohort.

	Non-ALI (N1 = 1,173)	ALI (N2 = 576)	*P* value
Demographic characteristics			
Age (years)	50 (40–58)	52 (44–61)	<0.001
Sex (male)	886 (75.5%)	413 (71.7%)	0.085
Height (cm)	172 (166–176)	170 (165–175)	<0.001
Weight (kg)	75 (65–83)	75 (65–85)	0.835
Body mass index (kg/m^2)	25.4 (22.9–27.8)	25.6 (23.5–28.5)	0.021
Clinical characteristics			
Time onset to operation (days)	1 (1–2)	1 (1–2)	0.532
Heart rate (bpm)	80 (75–85)	80 (76–88)	<0.001
Diastolic blood pressure (mmHg)	75 (68–80)	75 (67–80)	0.789
Systolic blood pressure (mmHg)	129 (120–139)	130 (119–140)	0.623
Mean blood pressure (mmHg)	93 (85–99)	93 (84–100)	0.941
Smoking *n* (%)	499 (43.2%)	239 (41.8%)	0.564
Drinking *n* (%)	226 (20.0%)	118 (21.1%)	0.594
Chronic lung disease *n* (%)	25 (2.1%)	12 (2.1%)	0.940
Coronary heart disease *n* (%)	116 (9.9%)	48 (8.3%)	0.292
Hypertension *n* (%)	800 (68.8%)	449 (78.1%)	<0.001
Diabetes *n* (%)	61 (5.2%)	29 (5.0%)	0.883
Arrhythmias *n* (%)	24 (2.1%)	22 (3.8%)	0.030
Congestive heart failure *n* (%)	3 (0.3%)	1 (0.2%)	0.735
Marfan syndrome *n* (%)	22 (1.9%)	4 (0.7%)	0.055
Dissection characteristics			
Malperfusion[a] *n* (%)	326 (27.8%)	234 (40.6%)	<0.001
Circulation characteristics			
Aortic regurgitation *n* (%)			<0.001
Mild	356 (31.6%)	197 (38.0%)	
Moderate	132 (11.7%)	83 (16.0%)	
Severe	241 (21.4%)	98 (18.9%)	
Pericardial effusion *n* (%)			0.006
Mild	103 (8.9%)	58 (10.1%)	
Moderate	13 (1.1%)	17 (3.0%)	
Severe	6 (0.5%)	8 (1.4%)	
Pleural effusion *n* (%)			0.121
Minor	42 (3.6%)	23 (4.0%)	
Major	23 (2.0%)	4 (0.7%)	
LVEDD (mm)	51 (47–56)	49 (45–54)	<0.001
LVEF (%)	62 (59–66)	62 (58–65)	0.191
LVESD (mm)	33 (30–37)	32 (28–36)	<0.001
Biomarkers			
Leukocyte (× 109/L)	7.8 (5.9–11.0)	10.3 (7.0–13.4)	<0.001
Platelet (× 109/L)	201 (162–246)	181 (144–223)	<0.001
Hemoglobin (g/L)	139.0 (127.0–150.0)	137.0 (122.0–147.0)	0.003
Creatine kinase-MB (ng/mL)	1.1 (0.7–2.0)	1.5 (0.9–3.0)	<0.001
Lactic dehydrogenase (U/L)	187 (161–228)	209 (173–255)	<0.001
Alanine transaminase (U/L)	19 (13–28)	20 (14.0–32)	0.010
Aspartate aminotransferase (u/L)	19 (15–25)	21 (17–32)	<0.001
Albumin (g/L)	40.8 (37.7–43.6)	39.5 (36.1–42.2)	<0.001
Blood urea nitrogen (mmol/L)	5.5 (4.6–7.1)	6.5 (5.0–8.3)	<0.001
Creatinine (μmoI/L)	72.2 (60.6–84.6)	78.8 (64.6–102.6)	<0.001
INR	1.07 (1.01–1.14)	1.08 (1.02–1.17)	0.003
APPT (s)	30.6 (28.3–33.2)	30.0 (28.0–32.4)	0.005
PH	7.42 (7.40–7.44)	7.42 (7.39–7.45)	0.989
$PaCO_2$ (mmHg)	35.2 (32.3–38.2)	34.7 (31.4–37.5)	0.009
Base excess (mmol/L)	−0.6 (−1.9 to 0.9)	−1.0 (−2.4 to 0.6)	<0.001
Glucose (mmol/L)	5.6 (4.9–7.0)	6.8 (5.5–8.0)	<0.001
Lactate (mmol/L)	1.3 (1.0–1.8)	1.4 (1.0–2.1)	0.006
Procedural variables			
Root procedure			0.269
Aortic root repair (%)	22 (1.9%)	14 (2.4%)	
Aortic valve replacement (%)	55 (4.7%)	18 (3.1%)	
Aortic root replacement (%)	458 (39.0%)	213 (37.0%)	
Bentall (%)	424 (36.1%)	204 (35.4%)	0.765
David (%)	23 (2.0%)	0 (0.0%)	<0.001
Total arch replacement + FET implantation (%)	483 (41.2%)	368 (63.9%)	<0.001
Hemi-arch replacement (%)	144 (12.3%)	76 (13.2%)	<0.001
Total arch replacement (%)	494 (42.1%)	370 (64.2%)	
Inclusion technique (%)	781 (66.6%)	475 (82.5%)	<0.001
Concomitant CABG (%)	79 (6.7%)	55 (9.5%)	0.038
Concomitant valve surgery (%)	53 (4.5%)	24 (4.2%)	0.736
Cardiopulmonary bypass time (min)	160 (129–195)	192 (158–224)	<0.001
Aortic cross-clamp time (min)	94 (72–118)	107 (88–133)	<0.001

(*continued*)

Table 2. Continued

	Non-ALI (N1 = 1,173)	ALI (N2 = 576)	P value
Circulatory arrest time (min)	23 (18–30)	23 (18–29)	0.597
Anti-inflammatory therapeutics			
Ulinastatin	474 (40.4%)	201 (34.9%)	0.026
Perioperative outcomes			
30-day mortality (%)	20 (1.7%)	51 (8.9%)	<0.001
Inhospital mortality (%)	21 (1.8%)	57 (9.9%)	<0.001
Mechanical ventilation time (h)	16 (12–18)	51 (37–111)	<0.001
ICU stay (h)	20 (17–35)	84 (45–156)	<0.001
Hospital stay (days)	15 (11–21)	16 (12–23)	0.037

Data are *n* (%) or median (IQR), unless otherwise specified.
ALI, acute lung injury; LVEDD, left ventricular end-diastolic dimension; LVESD, left ventricular end-systolic dimension; LVEF, left ventricular ejection fraction; INR, international normalized ratio; APTT, activated partial prothrombin time; FET, frozen elephant trunk; CABG, coronary artery bypass grafting; ICU, intensive care unit.
[a]Defined as one of the following conditions: coronary malperfusion, renal malperfusion, cerebral perfusion, spinal/lumbar, and intestinal and limb ischemia.

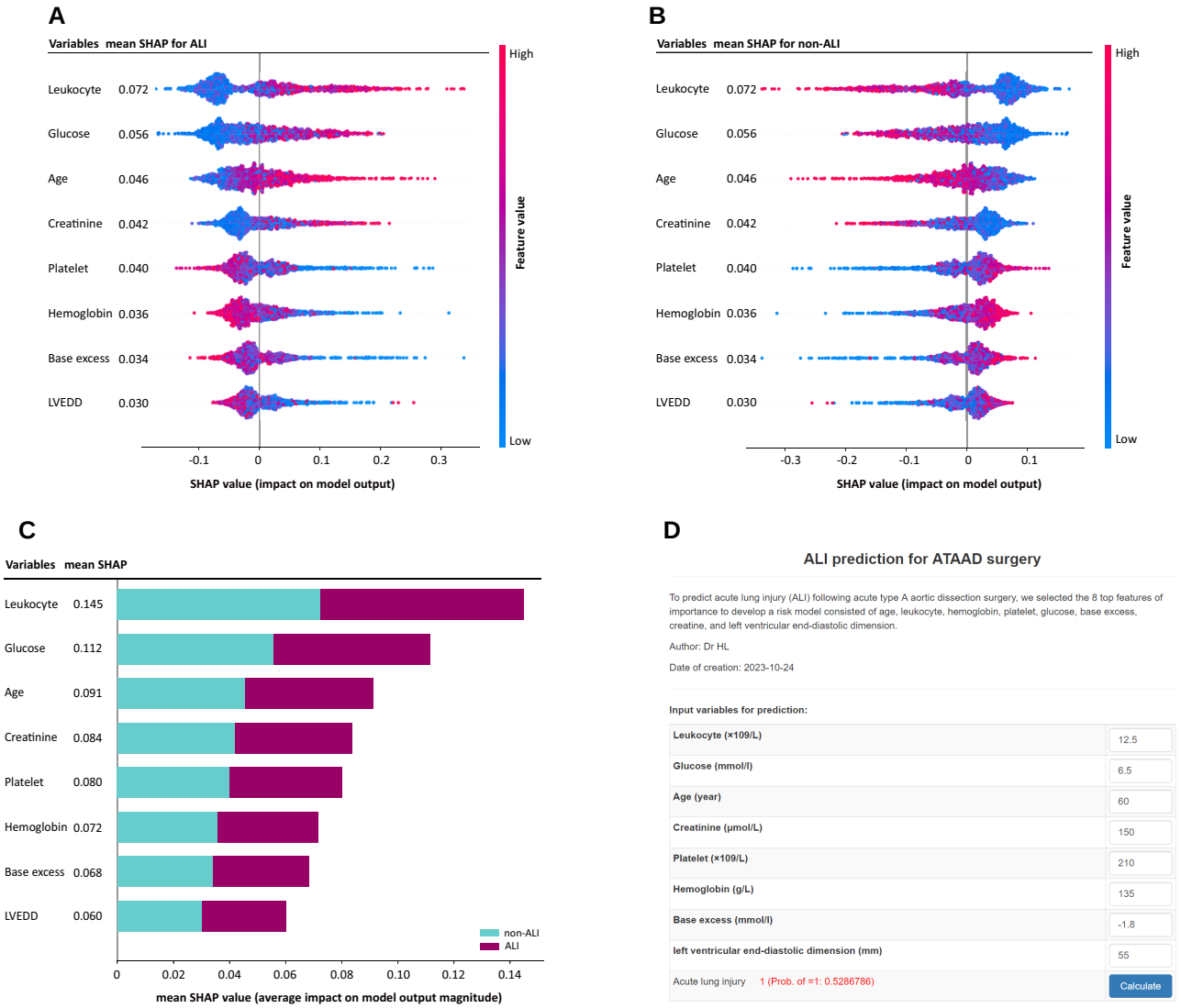

Fig. 1. Characteristics and schematics of simplified ALI risk model. A) SHAP plot of each predictor influencing non-ALI prediction, B) SHAP plot of each predictor influencing ALI prediction, C) summary plot of each predictor influencing ALI prediction, and D) the screenshot of the simplified model online calculator. LVEDD, left ventricular end-diastolic dimension.

associated with lower risk of developing ALI (241/1,074 [58.5%] vs. 122/675 [46.7%]; risk difference 0.24 [95% CI 0.08, 0.39]; OR 0.623 [95% CI 0.456, 0.851]; $P = 0.003$) in patients with a risk of 32.5–73.0%, rather than in patients with an ALI risk probability of <32.5% and >73.0% (134/1,074 [20.2%] vs. 79/675 [19.1%]; risk difference 0.03 [95% CI −0.09, 0.15]; OR 0.929 [0.682, 1.267], $P = 0.642$) (Pinteraction = 0.075) (Table 3). The multivariable analysis confirmed the significant association between ulinastatin use and ALI

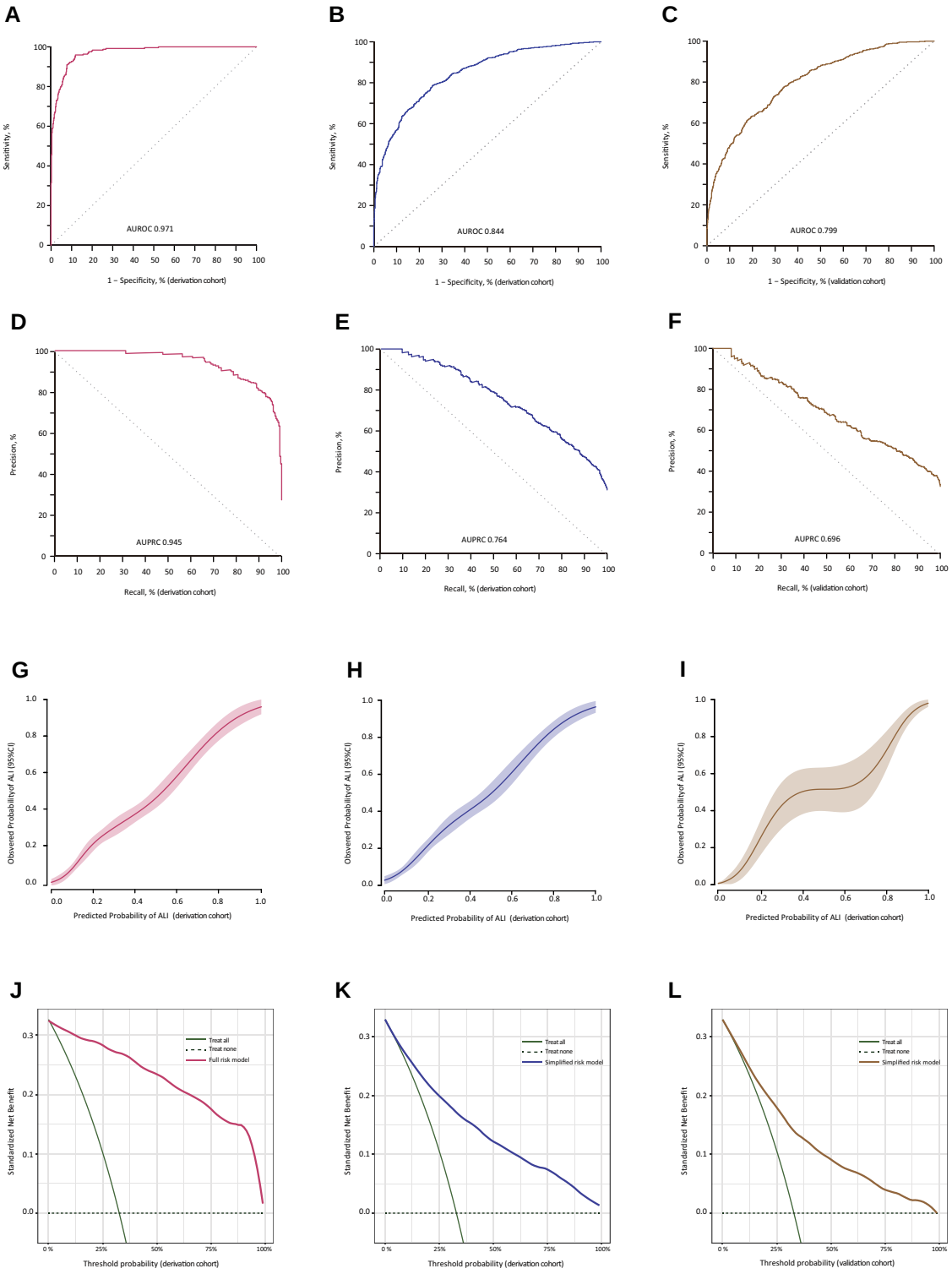

Fig. 2. AUROC and AUPRC of the ALI risk model in the derivation and validation cohorts. A, D) AUROC and AUPRC of the full ALI risk model in the derivation cohort; B, E) AUROC and AUPRC of the simplified ALI risk model in the derivation cohort; C, F) AUROC and AUPRC of the simplified ALI risk model in the validation cohort; G, I) calibration curve and decision curve of the full ALI risk model in the derivation cohort; H, J) calibration curve and decision curve of the simplified ALI risk model in the derivation cohort; I, L) calibration curve and decision curve of the simplified ALI risk model in the validation cohort. AUROC, area under the receiver operating characteristic curve; AUPRC, area under the precision-recall curve.

(adjusted OR 0.666; 95% CI 0.530, 0.836, $P = 0.0005$) (Pinteraction = 0.133) with adjustment for baseline, clinical procedural factors.

In derivation cohort, the estimated NNT was 19 (95% CI 11, 162) showing one patient being prevented from developing ALI in every 19 patients who have been treated with ulinastatin compared with those without ulinastatin. The estimated NNT was 9 (95% CI 5, 25) showing one patient being prevented from developing ALI in every nine patients who have been treated with ulinastatin among patients with a predicted risk of 32.5–73.0% compared with those without ulinastatin, however, no significant have no

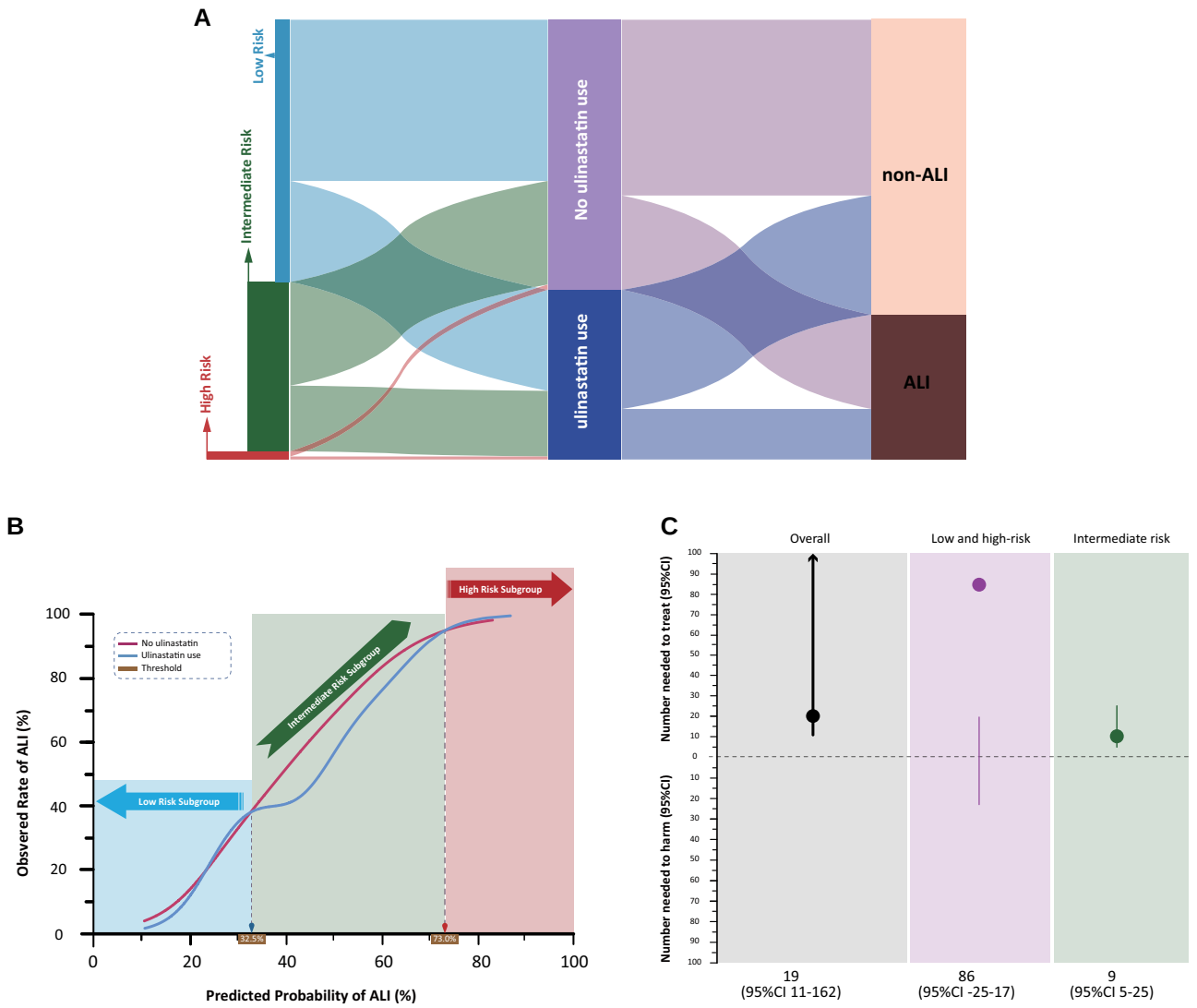

Fig. 3. Relationship between risk stratification and ulinastatin use in the derivation cohort. A) Alluvial plot showing distribution of risk stratifications across ulinastatin use and ALI; B) cubic splines of the predicted and observed risk of ALI by absence vs. presence of ulinastatin use; C) NNT/NNH of the absence vs. presence of ulinastatin use overall and in each risk stratification.

statistical differences between absence and presence of ulinastatin in patients with a risk probability of <32.5 or >73.0% (Fig. 3C).

The observed ALI rates varied substantially across risk groups: 180/1,043 (17.3%), 363/673 (53.9%), and 33/33 (100.0%) in the low, intermediate, and high-risk group, respectively (P for trend <0.001). With reference to the low-risk group, the intermediate group conferred significantly higher risk of ALI (crude OR 5.614 [95% CI 4.502, 7.002]; $P < 0.00001$; adjusted OR 4.890 [95% CI 3.841, 6.227]; $P < 0.001$).

Discussion

In this cohort of ATAAD patients from China, we have developed and confirmed a risk scoring model that predicted the risk of developing ALI after ATAAD surgery. This model exhibits satisfactory performance in terms of discrimination, calibration, and clinical usefulness in both the development and validation groups. Subgroup analysis showed that ulinastatin use was associated with a significantly lower risk of developing ALI in patients with a risk probability of 32.5–73.0%, but with similar risk of developing ALI in patients with a risk probability of <32.5 or >73.0%. These findings underline the importance of risk stratification to provide better individualized anti-inflammatory treatment for patients with ATAAD.

The mechanism by which ALI forms after ATAAD has not been completely elucidated; however, it is generally believed that inflammation plays an important role in the process (21, 22). High inflammatory biomarker such as C-reactive protein (CRP), interleukin-6, and leukocyte has been observed in patients as soon as the onset of the syndrome, indicating the early initiation of the inflammatory cascade at the very beginning of the development of aortic dissection, which have been confirmed to be related to perioperative mortality among patients with ATAAD (23–25).

However, the association between leukocyte count and ALI in patients with ATAAD remain unclear. In this study, we investigated the role of leukocyte in the development of ALI following ATAAD surgery. Unfortunately, CRP and IL-6 levels were not statistically analyzed due to their high missing rates. Based on SHAP analysis, we found that leukocyte was the top feature of importance among all the baseline and clinical covariates in predicting ALI after ATAAD surgery. In addition, an elevation in peripheral leukocyte count was associated with a higher risk of developing

Table 3. Comparison of outcome of interest between ulinastatin use or not use in derivation cohort.

	No ulinastatin	Ulinastatin	Risk difference (95% CI)	OR (95% CI)	P value	Adjusted OR[a] (95% CI)	P value[a]
Acute lung injury							
Overall, N = 1,749	375/1,074 (34.9%)	201/675 (29.8%)	0.11 (0.01, 0.21)	0.790 (0.642, 0.972)	0.026	0.666 (0.530, 0.836)	0.0005
Low and high-risk subgroup, *n*1 = 1,076	134/662 (20.2%)	79/414 (19.1%)	0.03 (−0.09, 0.15)	0.929 (0.682, 1.267)	0.642	0.736 (0.520, 1.041)	0.083
Intermediate risk subgroup, *n*2 = 673	241/412 (58.5%)	122/261 (46.7%)	0.24 (0.08, 0.39)	0.623 (0.456, 0.851)	0.003	0.578 (0.417, 0.801)	0.001
30-day mortality							
Overall, N = 1,749	41/1,074 (3.8%)	30/675 (4.4%)	0.03 (−0.06, 0.13)	1.172 (0.724, 1.896)	0.518	0.936 (0.551, 1.590)	0.807
Low and high-risk subgroup, *n*1 = 1,076	11/662 (1.7%)	7/414 (1.7%)	0.00 (−0.12, 0.13)	1.018 (0.391, 2.647)	0.971	0.545 (0.173, 1.715)	0.299
Intermediate risk subgroup, *n*2 = 673	30/412 (7.3%)	23/261 (8.8%)	0.06 (−0.10, 0.21)	1.231 (0.698, 2.169)	0.473	1.151 (0.625, 2.118)	0.652
Inhospital mortality							
Overall, N = 1,749	46/1,074 (4.3%)	32/675 (4.7%)	0.02 (−0.07, 0.12)	1.112 (0.701, 1.765)	0.651	0.924 (0.550, 1.553)	0.766
Low and high-risk subgroup, *n*1 = 1,076	15/662 (2.3%)	9/414 (2.2%)	0.01 (−0.12, 0.13)	0.959 (0.416, 2.211)	0.920	0.604 (0.208, 1.752)	0.353
Intermediate risk subgroup, *n*2 = 673	31/412 (7.5%)	23/261 (8.8%)	0.05 (−0.11, 0.20)	1.188 (0.676, 2.086)	0.549	1.106 (0.603, 2.026)	0.745

[a]Adjustment for baseline, clinical procedural factors.

ALI. Given that systemic inflammatory reactions played a vital role in initiation and development of ALI along with the onset and treatment of ATAAD (3–5, 26), it highlighted the importance and necessity of anti-inflammatory in the treatment and prevention of ALI in management of ATAAD (27).

Our findings showed that patients with a low and high risk of ALI (defined risk probability of <32.5 or >73.0%) will not benefit from ulinastatin use while patients with an intermediate risk of ALI (defined risk probability of 32.5–73.0%) will benefit from ulinastatin use, which indicates patients with a predicted ALI risk of 32.5–73.0% were likely to be the potential benefited population who had less risk probability of developing ALI after ATAAD surgery. These findings showed the significant heterogeneity of anti-inflammatory pharmacotherapy, which suggested individualized anti-inflammatory strategies in different risk probability of ALI. The clinical implications of our study hold significant importance. It is probable that individuals with varying risk probabilities exhibited diverse responses to anti-inflammatory pharmacotherapy, which could indicate variations in patient-specific risk profiles (10, 11). However, decision-making regarding ATAAD is complex in practice and requires weighing the benefits and risks of ulinastatin administration at the patient level. In addition, emerging immune-inflammatory properties including interleukins, non-coding RNA, and next-generation nanotechnology are being investigated and translated into medical therapies, which may indicate further advances in the pathologies of this catastrophic disease to improve treatment across in this area (28–30).

Strengths and limitations

This study benefits from a large sample size and multicenter nature. However, there are notable limitations worth discussing. First, one key limitation is the completeness of the datasets derived from clinical practice. Of note, the lack of information regarding genetic mutations especially for patients with aortopathies might compromise deep insight into the molecular mechanisms related to aortic dissection. Additionally, we did not analyze the relationship between the dose of ulinastatin and risk of ALI. Last, the study population was quite homogeneous, which may not reflect the diversity found in other countries and regions, which is likely to restrict the applicability of our findings to other healthcare settings.

Conclusion

In this study, we developed a data-driven machine learning-based risk scoring model to evaluate the treatment effect of anti-inflammatory pharmacotherapy (ulinastatin) in Chinese ATAAD patients. Our finding suggested that ATAAD patients with intermediate risk of ALI were likely to benefit from ulinastatin use, however, ATAAD patients with low and high risk of ALI were not likely to benefit from ulinastatin use. These discoveries emphasized the significance of risk stratification in more personalized treatment for individuals with ATAAD. The interpretation of our results is associated with a few limitations, which require further investigation in future studies.

Supplementary Material

Supplementary material is available at *PNAS Nexus* online.

Funding

This work was supported by Jiangsu Provincial Innovative & Entrepreneurial Talent Project, Outstanding Young Talent Support Plan Project of Jiangsu Provincial Hospital, and Public Welfare Project of Nanjing Medical University Alliance for Specific Diseases (JZ23349020230306).

Author Contributions

H.L. and S.Z. had the idea of the study, conceptualized the research aims; H.L. design the study and take responsibility for the integrity of the data and the accuracy of the data analysis, doing the statistical analysis, and wrote the first draft of the article; H.L., Y.F.D., S.C.Q., S.Z., H.Y.L., Y.F.S., and H.J.Z. contributed to the acquisition of data; and other authors provided comments and approved the final manuscript.

Data Availability

All data supporting the findings of this study are included in the main text and Supplementary material.

Ethics Approval

Patient written consent for the publication of the study data was waived by the IRB due to this retrospectively observational study.

References

1 Malaisrie SC, *et al.* 2021. 2021 The American Association for Thoracic Surgery expert consensus document: surgical treatment of acute type A aortic dissection. *J Thorac Cardiovasc Surg*. 162(3):735–758.e2.

2 Evangelista A, *et al.* 2018. Insights from the international registry of acute aortic dissection: a 20-year experience of collaborative clinical research. *Circulation*. 137:1846–1860.

3 Svyatets M, Tolani K, Zhang M, Tulman G, Charchaflieh J. 2010. Perioperative management of deep hypothermic circulatory arrest. *J Cardiothorac Vasc Anesth*. 24(4):644–655.

4 Arnaoutoglou E, *et al.* 2010. Post-implantation syndrome after endovascular repair of aortic aneurysms: need for postdischarge surveillance. *Interact Cardiovasc Thorac Surg*. 11(4):449–454.

5 Day JRS, Taylor KM. 2005. The systemic inflammatory response syndrome and cardiopulmonary bypass. *Int J Surg*. 3(2):129–140.

6 Luo MH, *et al.* 2022. Early postoperative organ dysfunction is highly associated with the mortality risk of patients with type A aortic dissection. *Interact Cardiovasc Thorac Surg*. 35(6):ivac266.

7 Morimoto N, *et al.* 2008. Sivelestat attenuates postoperative pulmonary dysfunction after total arch replacement under deep hypothermia. *Eur J Cardiothorac Surg*. 34(4):798–804.

8 Xu CE, Zou CW, Zhang MY, Guo L. 2013. Effects of high-dose ulinastatin on inflammatory response and pulmonary function in patients with type-A aortic dissection after cardiopulmonary bypass under deep hypothermic circulatory arrest. *J Cardiothorac Vasc Anesth*. 27(3):479–484.

9 Liu H, Qian SC, Shao YF, Li HY; Additive Anti-inflammatory Action for Aortopathy & Arteriopathy (5A) Investigators Group. 2022. Anti-inflammatory effect of ulinastatin on the association between inflammatory phenotypes in acute type A aortic dissection. *J Inflamm Res*. 15:3709–3718.

10 Liu H, *et al.* 2023. Inflammatory risk stratification individualizes anti-inflammatory pharmacotherapy for acute type A aortic dissection. *Innovation (Camb)*. 4(4):100448.

11 Liu H, Qian S-C, Li H-Y, Shao Y-F, Zhang H-J. 2024. Chinese Additive Anti-inflammatory Action for Aortopathy & Arteriopathy (5A) Registry protocol: rationale, design and methodology. *BMC Cardiovasc Disord*. 24(1):120.

12 Liu H, *et al.* 2024. Anti-inflammatory response-based risk assessment in acute type A aortic dissection: a national multicenter cohort study. *Int J Cardiol Heart Vasc*. 50:101341.

13 Collins GS, Reitsma JB, Altman DG, Moons KGM. 2015. Transparent reporting of a multivariable prediction model for individual prognosis or diagnosis (TRIPOD): the TRIPOD statement. *BMJ*. 350:g7594.

14 Sun L, Qi R, Zhu J, Liu Y, Zheng J. 2011. Total arch replacement combined with stented elephant trunk implantation: a new "standard" therapy for type a dissection involving repair of the aortic arch? *Circulation*. 123(9):971–978.

15 Marco Ranieri V, *et al.* 2012. Acute respiratory distress syndrome: the Berlin definition. *JAMA*. 307(23):2526–2533.

16 Matute-Bello G, *et al.* 2011. An official American Thoracic Society workshop report: features and measurements of experimental acute lung injury in animals. *Am J Respir Cell Mol Biol*. 44(5):725–738.

17 Chen T, Guestrin C. 2016. XGBoost: a scalable tree boosting system. Proceedings of the 22nd ACM SIGKDD International Conference on Knowledge Discovery and Data Mining; San Francisco, 13–17 August 2016. p. 785–794.

18 Lundberg SM, *et al.* 2020. From local explanations to global understanding with explainable AI for trees. *Nat Mach Intell*. 2(1):56–67.

19 Alba AC, *et al.* 2017. Discrimination and calibration of clinical prediction models: users' guides to the medical literature. *JAMA*. 318(14):1377–1384.

20 Vickers AJ, Elkin EB. 2006. Decision curve analysis: a novel method for evaluating prediction models. *Med Decis Making*. 26(6):565–574.

21 Sayed A, Munir M, Bahbah EI. 2021. Aortic dissection: a review of the pathophysiology, management and prospective advances. *Curr Cardiol Rev*. 17(4):e230421186875.

22 Bossone E, Eagle KA. 2021. Epidemiology and management of aortic disease: aortic aneurysms and acute aortic syndromes. *Nat Rev Cardiol*. 18(5):331–348.

23 Jenab Y, Ahmadi-Tafti SH, Davarpasand T, Jalali A, Khederlou H. 2023. Association of the high-sensitive cardiac troponin T levels and long-term mortality in patients with acute aortic dissection type A. *J Cardiovasc Thorac Res*. 15(2):116–120.

24 Wu Q, *et al.* 2020. Efficacy of interleukin-6 in combination with D-dimer in predicting early poor postoperative prognosis after acute Stanford type A aortic dissection. *J Cardiothorac Surg*. 15(1):172.

25 Liu H, *et al.* 2022. Circulating biomarker-based risk stratifications individualize arch repair strategy of acute type A aortic dissection via the XGBoosting algorithm. *Eur Heart J Digit Health*. 3(4):587–599.

26 Gorla R, *et al.* 2016. Clinical features and prognostic value of stent-graft-induced post-implantation syndrome after thoracic endovascular aortic repair in patients with type B acute aortic syndromes. *Eur J Cardiothorac Surg*. 49(4):1239–1247.

27 Nakanishi K, Takeda S, Sakamoto A, Kitamura A. 2006. Effects of ulinastatin treatment on the cardiopulmonary bypass-induced hemodynamic instability and pulmonary dysfunction. *Crit Care Med*. 34(5):1351–1357.

28 Carrel T, Sundt TM III, von Kodolitsch Y, Czerny M. 2023. Acute aortic dissection. *Lancet*. 401(10378):773–788.

29 Gu J, *et al.* 2016. Intestinal barrier dysfunction: a novel therapeutic target for inflammatory response in acute Stanford type A aortic dissection. *J Cardiovasc Pharmacol Ther*. 21(1):64–69.

30 Rimmer LJ, Moughal S, Bashir M. 2020. Immunological therapeutics in acute aortic syndrome. *Asian Cardiovasc Thorac Ann*. 28(8):512–519.